Thermal Stability of Corrugated Epitaxial Graphene Grown on Re(0001)

E. Miniussi,[1,2] M. Pozzo,[3] A. Baraldi,[1,2,*] E. Vesselli,[1,2] R. R. Zhan,[1,2] G. Comelli,[1,2] T. O. Menteş,[4] M. A. Niño,[4,5] A. Locatelli,[4] S. Lizzit,[4] and D. Alfè[3,6]

[1]*Physics Department and CENMAT, University of Trieste, Via Valerio 2, I-34127 Trieste, Italy*
[2]*Laboratorio TASC IOM-CNR, S.S. 14 Km 163.5, I-34149 Trieste, Italy*
[3]*Department of Earth Sciences, Department of Physics and Astronomy, TYC@UCL, and London Centre for Nanotechnology, University College London, Gower Street, London WC1E 6BT, United Kingdom*
[4]*Sincrotrone Trieste S.C.p.A., Strada Statale 14 Km 163.5, I-34149 Trieste, Italy*
[5]*Instituto Madrileño de Estudios Avanzados en Nanociencia (IMDEA Nanociencia), Cantoblanco, 28049 Madrid, Spain*
[6]*IOM-CNR, DEMOCRITOS National Simulation Centre, I-34100 Trieste, Italy*

(Received 24 February 2011; published 25 May 2011)

We report on a novel approach to determine the relationship between the corrugation and the thermal stability of epitaxial graphene grown on a strongly interacting substrate. According to our density functional theory calculations, the C single layer grown on Re(0001) is strongly corrugated, with a buckling of 1.6 Å, yielding a simulated C 1*s* core level spectrum which is in excellent agreement with the experimental one. We found that corrugation is closely knit with the thermal stability of the C network: C-C bond breaking is favored in the strongly buckled regions of the moiré cell, though it requires the presence of diffusing graphene layer vacancies.

DOI: 10.1103/PhysRevLett.106.216101 PACS numbers: 68.35.B−, 68.43.−h, 71.15.Mb

Graphene (GR)-substrate interaction and its thermally induced changes can significantly affect not only the electronic, chemical, and geometric but also the heat transport properties of the C layer [1]. Phonon scattering can be enhanced by interaction with the substrate [2], thus resulting in an increased thermal conductivity which can provide a solution to heat dissipation problems of electronic devices [3]. The interaction with the substrate can also play an important role in determining the operational stability and lifetime of GR [4]. Indeed, the high-temperature formation of lattice defects is a key issue to understand the thermally driven changes in the electronic properties, and the disruption of the sp^2 network.

In this respect, GR corrugation plays a fundamental role. In freestanding exfoliated GR, intrinsic ripples arising from out-of-plane vibrations have been invoked to explain the thermodynamic stability of this material [5–7]. Moreover, the high-temperature formation of periodic ripples in GR is regarded as a new way to tailor the transport properties of this extraordinary material [1].

Differently from the free-standing case, the actual extent of corrugation in epitaxial GR supported on transition metal (TM) surfaces, and the way it affects the temperature-dependent GR properties, is still largely debated [8–14]. In this case, the corrugation arises from the epitaxial stress induced by the lattice mismatch between the C layer and the substrate, which results in superstructures with nanometer-scale periodicity. While epitaxial GR is completely flat on Ni [15–17], and it exhibits just a small corrugation on Pt and Ir surfaces, to date no general consensus has been reached about the actual size of GR corrugation on Ru(0001) [18–24]. It is clear that the accurate determination of GR corrugation is a key point to shed light on the GR-substrate interaction: a small corrugation is interpreted as due to weak van der Waals forces, while a large corrugation typically reflects a strong chemical bonding. In this Letter we propose a new approach, based on the combination of photoelectron spectroscopy and density functional theory (DFT) calculations, to explore the corrugation in epitaxial GR grown on Re(0001) and its relationship with the thermal stability. As far as the C-TM interaction is concerned, Re lies in between Ru, which is regarded as a strongly interacting GR-substrate system, and *W*, where only carbides form at high temperature.

Similarly to what has been recently reported by Moritz *et al.* [24] for GR/Ru(0001), our results indicate that a strong buckling is present also for GR/Ru(0001). Unlike GR/Ir(111), which is only weakly corrugated and is stable up to very high temperatures, GR on Re(0001) starts to break up just above 1000 K. Our results indicate that the breakup of the C layer begins in the strongly buckled regions of the moiré unit cell, where C atoms are closer to the metal surface. More specifically, DFT calculations indicate that, while a GR layer is intrinsically very stable, it starts dissolving only upon high-temperature C-vacancy diffusion in the strongly interacting regions.

The experiments were carried out at the SuperESCA and Nanospectroscopy beam lines of the Elettra synchrotron radiation facility. The Re(0001) surface was cleaned by repeated oxidizing treatments, followed by annealing to 2000 K. Epitaxial GR was grown by chemical vapor deposition, by repeatedly heating up the crystal to 1090 K in a C_2H_4 background ($p = 5 \times 10^{-7}$ mbar).

The single-layer GR sheet displays a long-range order [see low energy electron microscopy (LEEM) images in Fig. 1(a)], forming only one type of rotational domain which extends over the whole sample surface. The micro-low energy electron diffraction (μ-LEED) pattern is shown in the inset of Fig. 1(b). It exhibits extra spots around the zero- and the first-order diffraction spots of the substrate, a clear fingerprint of a moiré structure. A line profile analysis reveals that the moiré cell is made of (10×10) GR unit cells over (9×9) Re unit cells.

These results provided the starting configuration for the theoretical simulations. The DFT calculations were performed with the VASP code [25], using the projector-augmented wave method [26,27], the Perdew-Burke-Ernzerhof exchange-correlation functional [28], and adopting an efficient extrapolation method for the charge density [29]. Single particle orbitals were expanded in plane waves, with a cutoff energy of 400 eV.

Top and side views of the calculated minimum energy geometry of a GR layer on Re(0001) are shown in Fig. 1(c), where the color scale reflects the separation between the C layer and the underlying substrate. The structure is obtained by overlaying a (10×10) GR sheet over a (9×9) Re(0001) supercell formed by 4 Re layers, using the Γ point only and relaxing the top two Re layers together with the carbon layer. In the resulting configuration, the GR sheet is strongly corrugated, with C-Re distances mainly distributed between 2.1 and 2.4 Å, but ranging up to 3.8 Å, according to the histogram reported in Fig. 1(d). These distances refer to the average position of the Re atoms in the first layer, which have themselves a corrugation of less than 0.1 Å. Interestingly, this structure strongly resembles that obtained by Moritz *et al.* [24] for the largely debated GR/Ru(0001) system.

In order to test the consistency of the calculated structure we followed an innovative approach based on the comparison between the experimental and the calculated C 1*s* core level spectrum of GR. Indeed, the C 1*s* spectral line shape is known to be strongly affected by the interaction between GR and the TM substrate beneath [8]. The measured C 1*s* spectrum exhibits two main components, shifted by ~700 meV, which can be viewed as the hallmark of a strongly interacting GR-substrate system, in analogy with what observed on Ru(0001) and Rh(111) [8]. Following the assignment proposed for these systems, we attributed the low binding energy (BE) component to the weakly interacting regions of GR and the peak at higher BE to the strongly interacting ones. Actually, the net distinction between "weakly" and "strongly" interacting regions should be questioned, since it may overshadow the presence of a manifold of components, characterized by a different degree of interaction with the metal beneath. In order to shed light on this issue, we computed the C 1*s* core level binding energy for each of the 200 C atoms in the moiré cell, including also final state effects. The results, presented in Fig. 2(b), show that the BEs of all components are distributed in the range 284.3–285.8 eV, with a clear dependence on the C-Re distance. More specifically, as can be seen in the structural model, where the color scale refers to the BE, the closer a C atom is to the surface, the higher is its BE. The spectrum was then fitted to a sum of 200 Doniach-Šunjič (DS) functions, which combine a Lorentzian width, reflecting the finite core-hole lifetime, with the asymmetry parameter, related to *e-h* pair excitations. The DS profile was convoluted with a Gaussian to account for phonon and instrumental broadening. The BE of each component was fixed to its calculated value [30]. The excellent agreement between experimental and

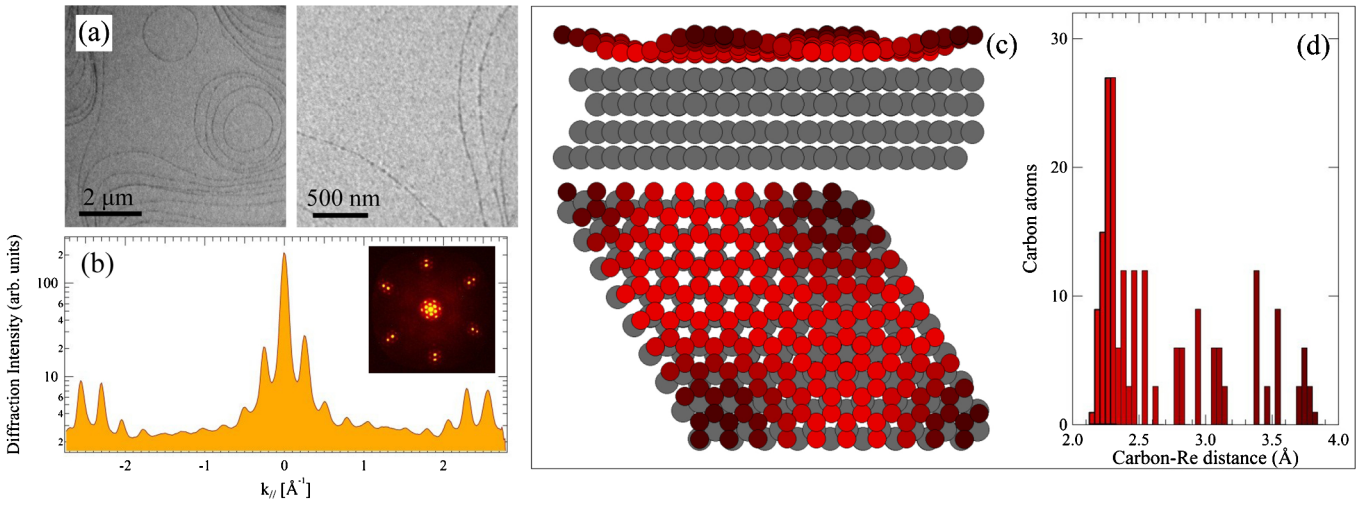

FIG. 1 (color online). (a) LEEM images at low (left) and high (right) magnification clearly show the homogeneity of the single-layer graphene film. The dark curved lines correspond to monoatomic steps of the substrate. (b) Line profile of the μ-LEED pattern of GR/Re(0001) (shown in the inset). (c) Top and side views of the simulated structure of GR/Re(0001). The color scale reflects the separation between C and the substrate beneath. (d) Distribution of the C-Re distances in the moiré cell.

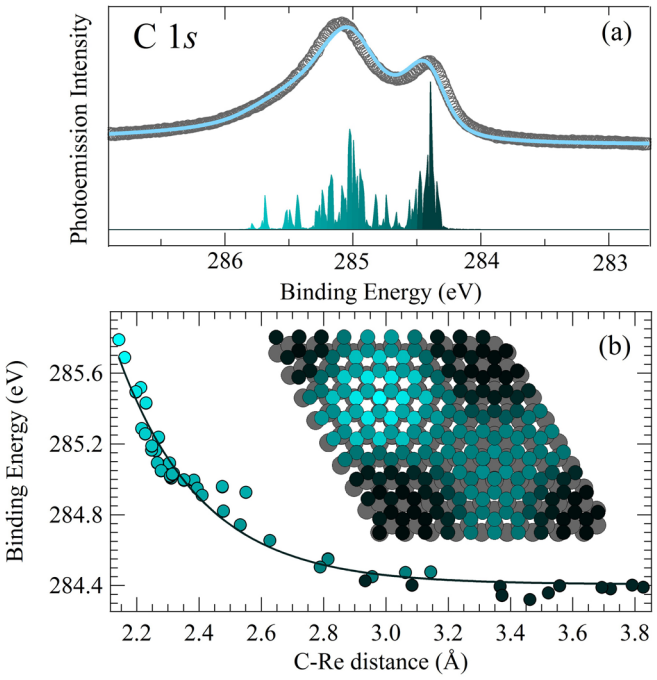

FIG. 2 (color online). (a) C 1s spectrum measured at normal emission and $h\nu = 400$ eV (empty circles) together with the simulated spectrum (solid line) and the calculated spectral distribution originated by the 200 C atoms. (b) BE of non-equivalent C atoms on the C-Re distance. The color scale in the model reflects the BEs of the different C 1s components.

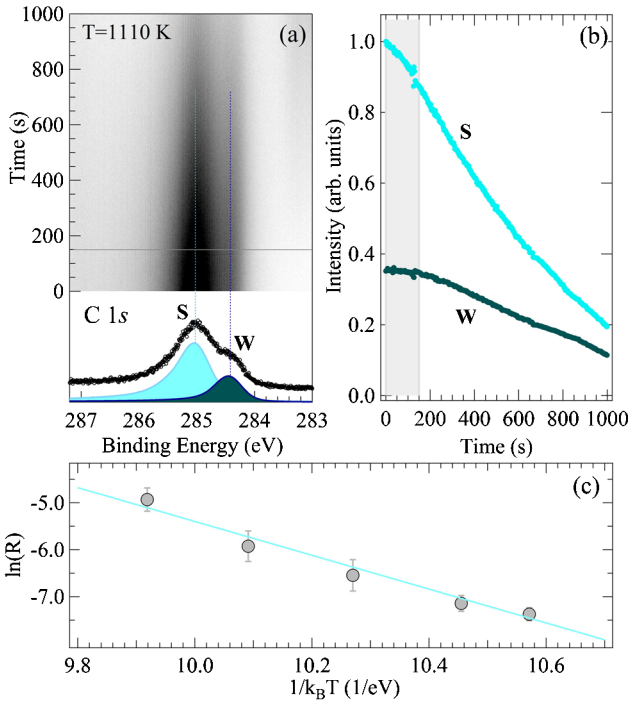

FIG. 3 (color online). (a) C 1s spectral evolution of the GR-covered sample at 1110 K. The components, associated to strongly and weakly interacting regions, are shown below the image plot. (b) Time evolution of the intensities of the S and W components. (c) Arrhenius plot of the decay rate of the S population.

simulated data, shown in Fig. 2(a), proves that the shape of the C 1s spectrum arises from an almost continuous, rather than binary distribution of C-Re distances.

The determination of GR corrugation served as a starting point to characterize its thermal stability. In order to address this issue, we monitored the evolution of the C 1s spectra at constant temperatures. The image plot in Fig. 3(a) shows the evolution of the C 1s spectrum at 1110 K. The initial stage ($t < 150$ s) is dominated by a depletion of the high BE component (S), which drops at a significantly faster rate with respect to the low BE component (W) [see Fig. 3(b)]. The overall C 1s signal is reduced, thus indicating that C dissolves into the bulk, rather than converting into different C species. The experiment was repeated at different temperatures, between 1095 and 1170 K. By fitting the decrease of the high BE component of the spectrum to an exponential we derived the temperature dependent decay rate of the C 1s signal, $R(T)$. Assuming that $R(T)$ depends on the activation energy for C-C bond breaking through a Boltzmann factor, we obtained the Arrhenius plot shown in Fig. 3(c), from which we estimated an effective barrier for C-C bond breakup and dissolution of 3.5 ± 0.7 eV.

In order to understand the initial microscopic mechanisms involved in the thermal breakup of the GR layer and its relationship with corrugation, we resorted to DFT to calculate the energy barriers, using the nudged elastic band (NEB) method [31]. The simplest mechanism one may think of involves a C atom being withdrawn from the GR network and migrating into the bulk. Starting from a defect-free GR layer, we found that the lowest-energy configuration for this path is obtained by removing a C atom from a strongly interacting region and placing it in a hollow subsurface interstitial site, leaving a hole almost on top of a Re atom. This final state yields an energy ~3 eV higher than that of the initial state, due to the high energetic cost of breaking three strong sp^2 planar bonds. The overall calculated energy barrier amounts to 6 eV, which is almost twice as large as the experimental one. This suggests that GR breaking follows a different path. Indeed, once a C monovacancy has formed, the cost of removing a carbon atom from one of the neighboring sites and displacing it below the surface is considerably lower, since it involves the breakup of only two sp^2 bonds. Following similar arguments, we believe that the pentagon-heptagon local arrangements, which have been found on SiC and involve only threefold coordinated C atoms [32], would have a larger barrier for breakup.

In the presence of a vacancy, the energy of the system increases by only ~0.8 eV, and the overall barrier is reduced to ~4 eV (see Fig. 4), which matches the experimental estimate. This suggests that, while a defect-free GR cannot break at the temperature we used, a defective one

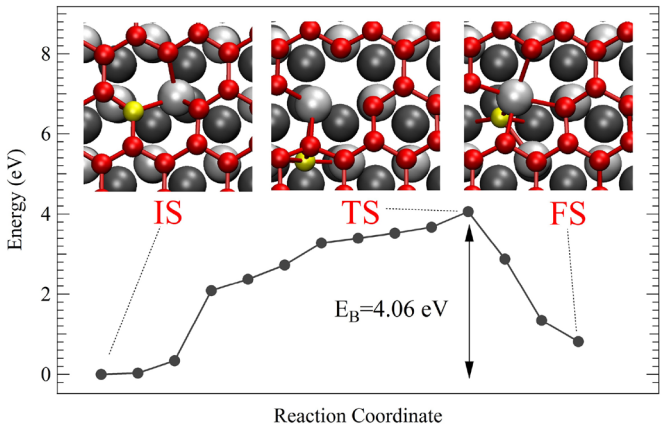

FIG. 4 (color online). Reaction path for GR layer breaking in the presence of a C vacancy in the strongly interacting region of the moiré cell as obtained from NEB simulations. Initial (IS), transition (TS), and final state (FS) structural geometries are shown.

can. The role of vacancy defects is indirectly supported by LEEM imaging, which rules out that the GR layer initial dissolution proceeds by reaction fronts starting at step edges or other macroscopic defects. Instead, GR seems to break up homogeneously within single terraces, on length scales well below few tens of nanometers. Diffraction line profile analysis provides further evidence that the average domain size remains constant during the initial phase of GR dissolution, indicating that the breakup involves the formation of point defects.

A final question remains to be answered: how is it possible to create vacancies in the interacting region? A realistic pathway would be the formation of vacancies at the domain boundaries formed during GR growth. Hence, the formation of vacancies in the strongly interacting region may be allowed by low energy barriers for their diffusion. We calculated these barriers for monovacancies, since divacancies turned out to have a higher diffusion barrier [33], and found that in the weakly interacting regions they amount to less than 1 eV. The barriers increase as the vacancy approaches the strongly interacting region, though never exceeding ~4 eV, which is comparable to the barrier for the subsurface penetration of a second C atom. Thus, we propose that the mechanism of GR breaking involves the presence of monovacancies, which quickly migrate to the strongly interacting regions where subsequent C-C bond breakup takes place.

In conclusion, we have shown that there is a close relationship between GR corrugation and its thermal stability, a key achievement in sight of the potential high-temperature applications of supported GR. Among the most appealing perspectives, we should mention the use of GR as a heat dissipator in a wealth of electronic devices or as protective layer under highly oxidizing conditions.

The work of D. A. and M. P. was conducted as part of a EURYI grant as provided by EPSRC. Calculations were performed on the HECToR national service (U.K.) and used resources of the Oak Ridge Leadership Computing Facility (National Center for Computational Sciences at Oak Ridge National Laboratory), which is supported by the Office of Science of the Department of Energy under Contract No. DE-AC05-00OR22725 (USA). D. A. and A. B. acknowledge the Royal Society for support. We thank K. Prince for fruitful discussions.

*alessandro.baraldi@elettra.trieste.it

[1] R. Miranda and A. Vazquez de Parga, Nature Nanotech. **4**, 549 (2009).
[2] J. Seol *et al.*, Science **328**, 213 (2010).
[3] R. Prasher, Science **328**, 185 (2010).
[4] K. Grosse *et al.*, Nature Nanotech. **6**, 287 (2011);
[5] C. Lui *et al.*, Nature (London) **462**, 339 (2009).
[6] J. Meyer, Nature (London) **446**, 60 (2007).
[7] A. Fasolino, J. Los, and M. Katsnelson, Nature Mater. **6**, 858 (2007).
[8] A. B. Preobrajenski, M. L. Ng, A. S. Vinogradov, and N. Mårtensson, Phys. Rev. B **78**, 073401 (2008).
[9] M. Gao *et al.*, Appl. Phys. Lett. **96**, 053109 (2010).
[10] K. Knox *et al.*, Phys. Rev. B **78**, 201408 (2008).
[11] U. Stoberl *et al.*, Appl. Phys. Lett. **93**, 051906 (2008).
[12] J. Wintterlin and M. Bocquet, Surf. Sci. **603**, 1841 (2009).
[13] M. Gibertini *et al.*, Phys. Rev. B **81**, 125437 (2010).
[14] V. Geringer *et al.*, Phys. Rev. Lett. **102**, 076102 (2009).
[15] G. Bertoni, L. Calmels, A. Altibelli, and V. Serin, Phys. Rev. B **71**, 075402 (2005).
[16] K. Yamamoto, M. Fukushima, T. Osaka, and C. Oshima, Phys. Rev. B **45**, 11358 (1992).
[17] Z. Xu and M. Buehler, J. Phys. Condens. Matter **22**, 485301 (2010).
[18] A. Vázquez de Parga *et al.*, Phys. Rev. Lett. **100**, 056807 (2008).
[19] D. Martoccia *et al.*, New J. Phys. **12**, 043028 (2010).
[20] D. Martoccia *et al.*, Phys. Rev. Lett. **101**, 126102 (2008).
[21] B. Wang, S. Günther, J. Wintterlin, and M. Bocquet, New J. Phys. **12**, 043041 (2010).
[22] B. Borca *et al.*, New J. Phys. **12**, 093018 (2010).
[23] X. Peng and R. Ahuja, Phys. Rev. B **82**, 045425 (2010).
[24] W. Moritz *et al.*, Phys. Rev. Lett. **104**, 136102 (2010).
[25] G. Kresse and J. Furthmüller, Phys. Rev. B **54**, 11 169 (1996).
[26] P. E. Blöchl, Phys. Rev. B **50**, 17 953 (1994).
[27] G. Kresse and D. Joubert, Phys. Rev. B **59**, 1758 (1999).
[28] J. P. Perdew, K. Burke, and M. Ernzerhof, Phys. Rev. Lett. **77**, 3865 (1996).
[29] D. Alfè, Comput. Phys. Commun. **118**, 31 (1999).
[30] See supplemental material at http://link.aps.org/supplemental/10.1103/PhysRevLett.106.216101 for further details.
[31] G. Henkelman, B. P. Uberuaga, and H. Jónsson, J. Chem. Phys. **113**, 9901 (2000).
[32] Y. Qi *et al.*, Phys. Rev. Lett. **105**, 085502 (2010).
[33] A. A. El-Barbary *et al.*, Phys. Rev. B **68**, 144107 (2003).